

This discussion paper is/has been under review for the journal *Atmospheric Chemistry and Physics (ACP)*. Please refer to the corresponding final paper in *ACP* if available.

**Elevated large-scale  
dust veil originated in  
the Taklimakan  
Desert**

K. Yumimoto et al.

# Elevated large-scale dust veil originated in the Taklimakan Desert: intercontinental transport and 3-dimensional structure captured by CALIPSO and regional and global models

K. Yumimoto<sup>1</sup>, K. Eguchi<sup>1</sup>, I. Uno<sup>1</sup>, T. Takemura<sup>1</sup>, Z. Liu<sup>2</sup>, A. Shimizu<sup>3</sup>, and N. Sugimoto<sup>3</sup>

<sup>1</sup>Research Institute for Applied Mechanics, Kyushu University, Fukuoka, Japan

<sup>2</sup>National Institute of Aerospace, Hampton, VA, USA

<sup>3</sup>National Institute for Environmental Studies, Tsukuba, Japan

Received: 22 April 2009 – Accepted: 24 June 2009 – Published: 3 July 2009

Correspondence to: K. Yumimoto (yumimoto@riam.kyushu-u.ac.jp)

Published by Copernicus Publications on behalf of the European Geosciences Union.

Title Page

Abstract

Introduction

Conclusions

References

Tables

Figures

⏪

⏩

◀

▶

Back

Close

Full Screen / Esc

Printer-friendly Version

Interactive Discussion

## Abstract

An intense dust storm occurred during 19–20 May 2007 over the Taklimakan Desert in northwestern China. In the following days, the space-borne lidar CALIOP tracked an optically thin, highly elevated, horizontally extensive dust veil that was transported intercontinentally over the eastern Asia, Pacific Ocean, North America, and Atlantic Ocean. A global aerosol transport model (SPRINTARS) also simulated the dust veil quite well and provided a 3-D view of the dust intercontinental transport. The SPRINTARS simulation revealed that the dust veil travels at 4–10 km altitudes with a thickness of 1–4 km along the isentropic surface between 310 K and 340 K. The transport speed is about 1500 km/d. The estimated dust amounts exported to the Pacific is 30.8 Gg, of which 65% is deposited in the Pacific and 18% is transported to the North Atlantic. These results imply that the dust veil can fertilize the open oceans, provide background dust to the atmosphere remote from the sources.

The entrainment mechanism that injects dust particles into the free atmosphere is important for understanding the formation of the dust veil and the subsequent long-range transport. We used a regional dust transport model (RC4) to analyze the dust emission and entrainment over the source region. The RC4 analysis revealed that strong northeasterly surface winds associated with a low pressure invade into the Taklimakan Desert through the east side corridor and form a strong up-slope wind along the high and steep mountainside of the Tibetan Plateau, blowing up large amounts of dust into the air. The updraft further brings the lofted dust particles up to the free troposphere (about 9 km MSL) where the westerly generally blows. The peculiar terrain surrounding the Taklimakan Desert plays the key role in the entrainment of dust to the free troposphere to form the dust veil.

ACPD

9, 14453–14481, 2009

## Elevated large-scale dust veil originated in the Taklimakan Desert

K. Yumimoto et al.

Title Page

Abstract

Introduction

Conclusions

References

Tables

Figures

⏪

⏩

◀

▶

Back

Close

Full Screen / Esc

Printer-friendly Version

Interactive Discussion

## 1 Introduction

Asian dust is well known to impact the regional and remote air quality and climate over the eastern Asia, the Pacific Ocean and beyond (Husar et al., 2001; McKendry et al., 2001; Yu et al., 2003). The Taklimakan Desert, which is located in the Tarim Basin with an area of  $\sim 320\,000\text{ km}^2$  bounded on three sides by high mountains (Fig. 1), is one of the largest deserts in the world. It is considered to be a major source of the dust transported into the North Pacific. Sun et al. (2001) suggested that dust materials from the Taklimakan Desert can be entrained to a high elevation ( $>5\text{ km}$ ) and transported over long distances by westerlies. Bory et al. (2003) compared the mineralogical and isotopic characteristics between the mineral dust deposit in northern Greenland and the samples from China and Mongolia, and suggested that the Taklimakan Desert is a primary source during the dusty spring. By analyzing three independent datasets (Nd isotopic composition measurement, back-trajectory and numerical model simulations), Grousset et al. (2003) suggested that the dust event observed on 6 March 1990 in the Alps is very likely an origin of the Taklimakan Desert. Matsuki et al. (2003) analyzed aircraft and lidar measurements and reported that the Taklimakan Desert is also an important source of the atmospheric background dust. However, direct observational evidences of the Asian dust intercontinental transport to Europe are useful to support these previous studies. In addition, the dust emission and entrainment processes in the Taklimakan Desert have not been investigated well, because of the complicated terrain and harsh climate which makes a long-term systematic study difficult using ground-based or airborne measurements. Especially, the uplifting mechanism of dust particles into the high troposphere over the Taklimakan Desert, which leads to the subsequent long-range transport, is required to be explored in more detail.

The long-range transport of dust particles affects the Earth's radiative budget both directly through scattering and absorbing the solar radiation (Bohren and Huffman, 1983) and indirectly by changing the cloud physical and radiative properties as the cloud condensation nuclei (Twomey, 1977). The transported dust also acts as a source of the

### Elevated large-scale dust veil originated in the Taklimakan Desert

K. Yumimoto et al.

Title Page

Abstract

Introduction

Conclusions

References

Tables

Figures

⏪

⏩

◀

▶

Back

Close

Full Screen / Esc

Printer-friendly Version

Interactive Discussion

nutrients to marine planktons in the upper waters through deposition (Martin et al., 1994), which in turn can influence the plankton and dimethyl sulfide (DMS) emissions (Duce et al., 1991). To estimate these effects accurately, extensive measurements of the dust transport altitudes, patterns and lifetime are required. Passive satellite observations (e.g., TOMS Aerosol Index and MODIS Aerosol Optical Thickness) have been providing useful information of the dust horizontal transport. However, an observation of 3-D distributions (particularly vertical structures) of the dust transport using these passive measurements is difficult.

The space-based lidar Cloud–Aerosol Lidar with Orthogonal Polarization (CALIOP) onboard the Cloud–Aerosol Lidar and Infrared Pathfinder Satellite Observation (CALIPSO) launched on 28 April 2006 provides new information of the global vertical distributions of aerosols and clouds (Winker et al., 2007). CALIOP has offered a unique opportunity to measure dust vertical distributions globally with the capability of depolarization ratio measurement. Based on the CALIOP observations, Liu et al. (2008a) presented a case of a large-scale dust plume which was originated in the Saharan Desert and transported across the North Atlantic into the Gulf of Mexico in the lower troposphere (<7 km) in 10 d. Seasonal 3-D distributions of the airborne dust over East Asia have been derived from the first year of the CALIOP measurements (Liu et al., 2008b). The dust distributions and seasonality are influenced significantly by the Tibetan Plateau with its particular orography. Huang et al. (2008) investigated the vertical structure of Asian dust based on the CALIOP observations during the Pacific Dust Experiment (PACDEX). However, there is difficulty in capturing the detailed 3-D structure and daily variations using the CALIOP measurement alone, because of the large longitudinal interval between two consecutive CALIPSO orbits (~1000 km at mid-latitude). Comprehensive studies are required for each of dust sources to understand their role in the Asian dust generation and transport. Very recently, Uno et al. (2008), Generoso et al. (2008), and Eguchi et al. (2009) performed integrated analyses using the CALIOP measurements and numerical model simulations and have provided more detailed 3-D structures of Asian dust and Saharan dust transports.

---

## Elevated large-scale dust veil originated in the Taklimakan Desert

K. Yumimoto et al.

---

Title Page

Abstract

Introduction

Conclusions

References

Tables

Figures

⏪

⏩

◀

▶

Back

Close

Full Screen / Esc

Printer-friendly Version

Interactive Discussion

---

**Elevated large-scale dust veil originated in the Taklimakan Desert**K. Yumimoto et al.

---

[Title Page](#)[Abstract](#)[Introduction](#)[Conclusions](#)[References](#)[Tables](#)[Figures](#)[⏪](#)[⏩](#)[◀](#)[▶](#)[Back](#)[Close](#)[Full Screen / Esc](#)[Printer-friendly Version](#)[Interactive Discussion](#)

An intensive dust storm occurred on 19–20 May 2007 in the Taklimakan Desert. On the following days, CALIOP detected an optically thin, highly lofted, extensive dust layer transported across over the eastern Asia, Pacific Ocean, North America, and the Atlantic Ocean. We name this type of dust layer as “dust veil” featured by its vertically thin and horizontally extensive structure. In this study, we perform a comprehensive investigation on the emission and entrainment procedures over the source region, the subsequent intercontinental transport, and 3-D structures of this dust veil, by combining regional and global aerosol transport models, in situ measurements, and passive and active satellite observations.

The models and observation data used in this study are described in Sect. 2. The global transport and 3-D structure of the dust veil are presented in Sect. 3, along with a detailed analysis of the dust emission and entrainment procedures in the Taklimakan Desert with a regional dust model. Our conclusions are presented in Sect. 4.

## 2 Numerical models and observation datasets

### 2.1 Numerical models

We use global and regional numerical models in our analyses. The regional model (with finer horizontal and vertical resolutions) is used for a detailed analysis of the emission and entrainment of the dust veil in the Taklimakan Desert. The subsequent intercontinental transport of the dust veil is analyzed using the global aerosol transport-radiation model.

The global aerosol transport-radiation model SPRINTARS (Takemura et al., 2005) used in this study is coupled interactively with an atmosphere–ocean general circulation model, MIROC (K-1 Model Developers, 2004). SPRINTARS includes explicit estimates of the direct, first indirect, and second indirect effects of aerosols. The horizontal resolution is T106 with 56 layers in a sigma coordinate. To focus on the transport of the dust veil originated in the Taklimakan Desert, only the emission of mineral dust

from the Taklimakan Desert (no dust emissions from the Gobi Desert, Mongolia, or Inner Mongolia regions) is taken into account.

The RAMS/CFORS-4DVAR regional dust transport model (RC4: Yumimoto et al., 2007, 2008) is applied to analyze the dust veil generation over the source region. RC4 is based on a successful dust model RAMS/CFORS (Uno et al., 2004). The RC4 domain is located over the eastern Asia (Fig. 1), with a horizontal resolution of 40 km, and 55 vertical stretching layers from the surface to 20 km (a vertical resolution of 140 m at the surface and 400 m at the top). To investigate the dust veil origin, dust emissions are limited to those over the Taklimakan Desert. In addition to the sensitive RC4 simulation, modeled wind fields, which RAMS/CFORS reproduces, are used for a 3-D particle simulation to investigate how dust particles are brought up to high altitudes to form the dust veil. In the particle simulation, the dust particles are emitted from the surface when the surface wind speed in the Taklimakan Desert becomes greater than 6.5 m/s (the number of emitted particles is proportional to the cube of the surface wind speed), and the emitted dust particles are transported by the modeled wind fields. The threshold wind speed and the third power-law relation are based on the analyses including surface observations (e.g. Kurosaki and Mikami, 2003) and numerical models (e.g., Tegen and Fung, 1994; Takemura et al., 2005).

Both the regional and global model simulations are nudged by the  $2.5^{\circ} \times 2.5^{\circ}$  NCEP/NCAR reanalysis data with a time interval of 6 h. The reanalysis data is also used for meteorological boundary conditions of the RAMS regional model.

## 2.2 Observation data

### 2.2.1 CALIOP

The space-based lidar CALIOP launched on 28 April 2006 onboard CALIPSO provides vertical distributions of aerosol and clouds on a global scale (Winker et al., 2007). In this study, for comparison with the model simulations we retrieve vertical profiles of the dust extinction coefficient from the total attenuated backscatter contained in the Level

## Elevated large-scale dust veil originated in the Taklimakan Desert

K. Yumimoto et al.

Title Page

Abstract

Introduction

Conclusions

References

Tables

Figures



Back

Close

Full Screen / Esc

Printer-friendly Version

Interactive Discussion

1B CALIOP data (ver. 2.01), using Fernald's inversion (Fernald, 1984) by setting the lidar ratio  $S1=50$  sr (Shimizu et al., 2004). Then, the retrieved vertical profiles are averaged into the CALIOP Level 2 data's horizontal resolution (5 km). The cloud-aerosol discrimination (CAD) index in the Level 2 CALIOP data is used for cloud layer detections. The methods used in this study for the CALIOP data processing are identical to those of Uno et al. (2008), Hara et al. (2009), and Eguchi et al. (2009).

## 2.2.2 NIES Lidar network

The NIES Lidar network (Shimizu et al., 2008) has 21 routine lidar observation sites distributed over Japan, Korea, China, Mongolia, and Thailand. It provides vertical profiles of aerosols and clouds with a high temporal resolution (15 min). The NIES lidar observation results are displayed in real time at <http://soramame.taiki.go.jp/dss/kosa/> and also used for inverse modeling of Asian dust in conjunction with a numerical model (Yumimoto et al., 2007, 2008). The detailed description of the NIES lidar data processing can be found in Shimizu et al. (2004).

## 2.2.3 Other observations

We also use the Ozone Monitoring Instrument (OMI) Aerosol Index (AI) measurement to examine the horizontal distributions of dust loading over the source region. The OMI AI represents a semi-quantitative estimate of columnar aerosol loading in a given pixel. A positive AI value indicates the existence of UV-absorbing aerosols (Prospero et al., 2002). The WMO SYNOP data (wind speed, wind direction, visibility and weather) are also used to investigate the emission of dust in the Taklimakan Desert.

# Elevated large-scale dust veil originated in the Taklimakan Desert

K. Yumimoto et al.

Title Page

Abstract

Introduction

Conclusions

References

Tables

Figures

⏪

⏩

◀

▶

Back

Close

Full Screen / Esc

Printer-friendly Version

Interactive Discussion

### 3 Results and discussion

#### 3.1 Intercontinental transport

As shown in Fig. 2a, CALIOP captures a very thin, highly elevated, large-scale dust veil that is originated in the Taklimakan Desert (green-yellowish features at high altitudes in the vertical transections of the CALIOP extinction coefficients). The dust veil is transported eastward from the Taklimakan Desert to the North Atlantic Ocean during 20–31 May 2007. Corresponding vertical transections of the model simulated dust extinction coefficients are presented in Fig. 2c, where the four transections over the eastern Asia during 21–24 May are derived from RC4 and the rest from SPRINTARS. Two models together track the dust veil transcontinental transport quite well. Figure 2b shows the HYSPLIT forward and backward trajectories (Draxler and Hess, 1998). The trajectories corroborate the long journey of the dust veil from the Taklimakan Desert, across over the North Pacific and North America, and into the North Atlantic Ocean.

Two panels in Fig. 3b present vertical cross-sections of the dust extinction coefficients measured by CALIOP and simulated by the RC4 model along the CALIPSO track on 23 May in Fig. 3a. The NIES lidar at Nagasaki (129.98° E, 32.94° N) also detected a 1-km-thick dust veil passing over at 6–7 km altitudes during the night of 23–24 May (left panel in Fig. 3c). For comparison, the RC4 simulated dust extinction coefficients for the same location and time period as the NIES lidar measurement is presented in the right panel of Fig. 3c. The height, thickness, and passage time of the dust measured by the NIES lidar are consistent with those measured by CALIOP. The RC4 model has captured similar characteristics of the dust veil.

Figure 4a shows longitudinal cross-section of the SPRINTARS dust extinction coefficient and potential temperature along the HYSPLIT trajectory from the Taklimakan Desert to the North Atlantic Ocean. Figure 4b (lower panels) presents comparison of averaged vertical profiles of dust extinction coefficients along the CALIOP orbit paths at ~145° E (eastern Asia), 5° W (the date line), and 70° W (Atlantic Ocean).

The SPRINTARS dust extinction coefficient (Fig. 4a) shows that the dust veil formed

## Elevated large-scale dust veil originated in the Taklimakan Desert

K. Yumimoto et al.

Title Page

Abstract

Introduction

Conclusions

References

Tables

Figures

⏪

⏩

◀

▶

Back

Close

Full Screen / Esc

Printer-friendly Version

Interactive Discussion



over the Taklimakan Desert is transported eastward at 5–10 km along the isentropic surface of 310–340 K over eastern Asia. CALIOP observed a thin dust layer of < 1 km on 24 May (the left panel of Fig. 4b; also see Fig. 2); however models are unable to capture the fine structure of the dust layer because of their insufficient vertical resolution. Comparing with the CALIOP and RC4 profiles, the center of the dust layer simulated by SPRINTARS is transported at a lower altitude, which may reflect that the global model with a coarser resolution cannot properly represent the wildly changing surface elevation and the complicated terrain over the source and the surrounding regions which plays an important role in the entrainment of dust particles into the free troposphere (described further in Sect. 3.2). However, SPRINTARS simulates dust altitudes reasonably well far away from the source region (see the middle and right panels in Fig. 4b).

The SPRINTARS simulation shows that the dust veil travels at 4–9 km altitudes with a thickness of 1–4 km and horizontally at 30–40° N over the Pacific Ocean (also see Fig. 2). The HYSPLIT forward trajectory (Fig. 2b) produces a dust pass over the western Pacific more northern and higher than both the CALIOP observation and the SPRINTARS simulation. Comparison of vertical profiles near the date line (the center panel of Fig. 4b) shows that the SPRINTARS simulation captures the dust veil quite well.

The dust veil reaches the west coast of North America during 28–29 May at 4–10 km (also see Fig. 2: 28 May-110044 and 29 May-100512 orbits). The dust veil is entrained into the lower troposphere and might have impacted the local air quality over the North America. On 31 May (Fig. 2: 31 May-063507 orbit), both CALIOP and SPRINTARS detect the dust veil over the North Atlantic Ocean vertically at 2–6 km and horizontally at 25–40° N (about 1700 km). Compared to that over the eastern Asia, the dust veil becomes more scattered vertically because of the deposition and diffusion of the dust particles (also see Fig. 4b). Grousset et al. (2003) reported that the Asian dust plume emitted in China on 25 February 1990 might have merged with the dust cloud transported from the Sahara Desert over Europe. We were unable to find a clear

## Elevated large-scale dust veil originated in the Taklimakan Desert

K. Yumimoto et al.

Title Page

Abstract

Introduction

Conclusions

References

Tables

Figures

⏪

⏩

◀

▶

Back

Close

Full Screen / Esc

Printer-friendly Version

Interactive Discussion

evidence of the dust veil studied in this paper mixed with the Saharan dust from the CALIOP measurements, SPRINTARS results, and HYSPLIT trajectory analysis.

The dust veil takes 12 days (20–31 May; also see HYSPLIT trajectories in Fig. 2b) to reach the North Atlantic Ocean from the dust source region, corresponding to a transport speed of  $\sim 1500$  km/d, consistent with Grousset et al. (2003) (20 000 km in two weeks based on a trajectory analysis) and Eguchi et al. (2009) (2000 km/d). The intercontinental transport of the dust veil brings mineral dust particles to the remote atmospheres and open oceans far away from the source region. The SPRINTARS simulation estimates a dust inflow to the Pacific Ocean (at  $130^\circ$  E) of 30.8 Gg, of which 65% is deposited in the Pacific Ocean (between  $140^\circ$  E and  $130^\circ$  W), and 18% is transported into the North Atlantic Ocean (at  $80^\circ$  W), as portrayed in Fig. 4a. This fact implies that the dust veil can play an important role in fertilizing the open oceans, providing background dust aerosol, and affecting the radiative budget through its absorption and scattering of the solar radiation.

Both the global and regional numerical models successfully capture the intercontinental transport of the dust veil, consistent with the CALIOP measurements and HYSPLIT trajectories, though they generally underestimate dust extinction coefficients (Fig. 2). The Taklimakan Desert is located in the Tarim Basin, surrounded on three sides by high mountains (see Fig. 1), which complicates the meteorological modeling inside the basin (Uno et al., 2005). The horizontal resolutions of both models may be insufficient to capture the sharply changing terrain, detailed wind fields, and dust emission. This may be one cause for the underestimation of dust emissions in our model simulations. The observed dust veil shows a small thickness of 1–2 km from the eastern Asia to the Pacific Ocean. The vertical resolutions of both models also may be still too coarse to reproduce such a fine structure and may be another cause for the underestimation of dust extinction coefficients.

---

## Elevated large-scale dust veil originated in the Taklimakan Desert

K. Yumimoto et al.

---

[Title Page](#)[Abstract](#)[Introduction](#)[Conclusions](#)[References](#)[Tables](#)[Figures](#)[Back](#)[Close](#)[Full Screen / Esc](#)[Printer-friendly Version](#)[Interactive Discussion](#)

### 3.2 Emission and entrainment processes of the dust veil

The dust emission and entrainment into the air over the source region are very important for the formation of the dust veil and its subsequent long-range transport. We perform a comprehensive analysis to investigate these processes using multiple measurement datasets and analysis tools. Figure 5 presents the meteorological conditions over the Tarim Basin from the RC4 regional model simulation for a time period of 17–22 May during which the dust veil forms. Also shown are the RC4 simulated dust particles emitted from the surface (right panels) and the OMI AI measurement (left panels), which is an indicator of the presence of absorbing aerosols (i.e. the dust over the source regions). Figure 6 shows the RC4 simulated and the SYNOP reported surface wind speed and direction at three SYNOP stations of Alar, Tazhong, and Ruoqiang located, respectively at the northern, middle, and eastern part of the Taklimakan Desert as indicated by the letters of A, T and R in Fig. 5. The SYNOP visibilities and RC4 surface dust concentrations are also shown.

As seen in Fig. 5a, a low pressure ( $L_1$ ) is generating on 17 May in North Mongolia, and strong northern winds are produced over the northern side of the Tarim Basin. On this day the air inside the basin is still calm. The RC4 simulation shows that only a small amount of dust particles is emitted from the surface in the basin (the right panel in Fig. 5a). The three SYNOP stations report weak surface winds ( $\leq 3$  m/s; not shown).

On 18 May (Fig. 5b), the cold northerly surface winds associated with the low pressure  $L_1$  become stronger over the northwestern China and, forced by the Tibetan Plateau, they change the direction and blow into the basin along the corridor on the eastern side. Meanwhile, a cold front forms over Mongolia, as indicated by the black line in the left panel of Fig. 5b. The OMI measurement shows a still low AI level over the desert. The particle simulation (the right panel in Fig. 5b) shows that the strong surface wind starts to sweep a significant amount of dust particles into the air and the top of the dust plume reaches the height of the Tibetan Plateau. At the SYNOP stations, both the wind speed and direction change suddenly and a strong northeasterly wind forms

## Elevated large-scale dust veil originated in the Taklimakan Desert

K. Yumimoto et al.

Title Page

Abstract

Introduction

Conclusions

References

Tables

Figures

⏪

⏩

◀

▶

Back

Close

Full Screen / Esc

Printer-friendly Version

Interactive Discussion

in the basin (Fig. 6), consistent with the RC4 simulated wind fields.

On 19 May (Fig. 5c), the strong wind blasts toward the southern side of the basin and produces upslope winds (about 0.2 m/s in the vertical direction). The windblown particles from the surface are then brought up to the free atmosphere by the upward wind along the northern slope of the Tibetan Plateau. The OMI AI becomes larger over the basin. The SYNOP stations, except the northern station at Alar, report strong surface winds (>5 m/s) and low visibilities (<3 km). Particularly at Ruoqiang, a considerably low visibility (<1 km) persists for 15 h.

On 20 May (Fig. 5d), strong surface wind continues to inject dust particles into the atmosphere. The OMI AI shows that dense dust spreads over the entire basin. The uplifted particles reach an altitude of ~9 km and are captured within the potential temperature zone of 320–340 K, where they are subsequently transported eastward by the strong westerly wind (>20 m/s) and start their intercontinental travel. The SYNOP stations report that strong surface winds (>5 m/s) persist over the basin on this day. Following the low pressure  $L_1$ , another low pressure ( $L_2$ ) appears north of the basin.

On 21 May (Fig. 5e), the OMI AI shows that most of the dust loading has been transported eastward out of the basin. At Tazhong (center) and Ruoqiang (east), the wind direction changes quickly from easterly to westerly. The SYNOP reports record a rain weather over the basin.

On 22 May (Fig. 5f; also see Fig. 7b), the OMI AI indicated that the dust has been transported to Mongolia and become weaker. Meanwhile, another dust storm is occurring in the basin, associated with the second low pressure ( $L_2$ ). This dust storm appears to be weaker than the first one that produced the dust veil. The SYNOP stations observe higher visibilities over the basin ( $\geq 6$  km).

Aoki et al. (2005) classified the mesoscale cold wind that produces dust storms in the Tarim Basin into three patterns. The wind that produced the dust veil studied in this paper may be identified as Pattern 1. This pattern is characterized by an easterly mesoscale wind turning its direction to westward along the eastern side corridor of the basin (compare Figs. 6 and 3 in Aoki et al., 2005). Eguchi et al. (2009) reported

## Elevated large-scale dust veil originated in the Taklimakan Desert

K. Yumimoto et al.

Title Page

Abstract

Introduction

Conclusions

References

Tables

Figures

⏪

⏩

◀

▶

Back

Close

Full Screen / Esc

Printer-friendly Version

Interactive Discussion

another case of long-range transport of a Taklimakan dust occurring during 8–10 May 2007 that belonged to Pattern 1. The special terrain of high and steep mountainside of the Tibetan Plateau on the southern side of the basin plays the key role in forming the strong updraft that carries dust particles into the upper troposphere for the long-range transport along the westerly.

To investigate the evolution of the dust veil transport in the free troposphere during the first few days, Fig. 7 shows a day-by-day overview of the RC4 simulated dust aerosol optical depth (AOD), wind field, potential temperature, center locations of the low pressures, and cloud distribution observed by MODIS/AQUA over the eastern Asia. Longitudinal-vertical transections of the RC4 dust extinction coefficients and the potential temperature are also shown. Note that the RC4 simulation shown in Fig. 7 allows only the dust emission from the Taklimakan Desert.

On 21 May (Fig. 7a), dust particles are injected into the free atmosphere, reaching an altitude of 9 km MSL at 04:00 UTC (also see Fig. 5). At ~19:00 UTC, CALIOP passed over the Gobi Desert (Fig. 2a: 21 May-190843 path) and detected two dense dust layers. One dust layer is near the surface. The other one is at 6–10 km altitudes. The RC4 simulation (Fig. 2c: 21 May-190843 path), which only considers dust emissions from the Taklimakan Desert, reproduces only one dust layer at higher altitudes, indicating that the upper dust layer observed by CALIOP is a Taklimakan Desert origin. The lower one should be generated in the other sources (very likely the Gobi Desert).

On 22 May, the modeled dust speeds up the eastward transport within the westerly (middle panel of Fig. 7b; also see passive satellite measurement in Fig. 5f). The vertical cross-section (lower panel in Fig. 7b) shows that the dust loading is transported across the Altun Shan Mountains at the northeastern Tibetan Plateau (see Fig. 1) with a thin structure within a potential temperature zone of 320–340 K. CALIOP (Fig. 1a: 22 May-181306 path) also detected a thin dust layer at 6–12 km on this day.

On 23 May (Fig. 7c), the low pressure  $L_2$  is in its deepening stage and forming a cold front over the Gobi deserts. The modeled AOT horizontal distribution (upper and middle panels in Fig. 7c) shows that the dust veil is transported in front of the

## Elevated large-scale dust veil originated in the Taklimakan Desert

K. Yumimoto et al.

Title Page

Abstract

Introduction

Conclusions

References

Tables

Figures

⏪

⏩

◀

▶

Back

Close

Full Screen / Esc

Printer-friendly Version

Interactive Discussion

---

## Elevated large-scale dust veil originated in the Taklimakan Desert

K. Yumimoto et al.

---

Title Page

Abstract

Introduction

Conclusions

References

Tables

Figures

⏪

⏩

◀

▶

Back

Close

Full Screen / Esc

Printer-friendly Version

Interactive Discussion



$L_2$  cold front extending in the north–south direction through the meandering westerly. The vertical cross-section (lower panel in Fig. 7c) demonstrates that the lower part of the dust remains behind the  $L_2$  cold front near  $115^\circ$  E, whereas the upper part of the dust (i.e. the dust veil) is transported beyond the cold front. This indicates that the dust veil at the free troposphere can travel faster than lower dust cloud (e.g. the Gobi dust transported typically at lower altitudes  $<5$  km). Eguchi et al. (2009) reported a Taklimakan dust layer that was transported at  $\sim 10$  km and could catch up with a Gobi dust layer generated 5 d earlier, forming a two-layered dust distribution over the eastern North Pacific.

On 24 May (Fig. 7d), the dust veil is transported farther between  $L_2$  and  $L_1$  along the westerly with its front part reaching Japan. The cross-section shows that the dust veil travels at 6–11 km altitudes within the isentropic surface of potential temperature of 320–340 K. In the following days, the dust veil continues its long journey to the North America and the North Atlantic, as discussed in previous subsection.

#### 4 Concluding remarks

CALIOP onboard the CALIPSO satellite tracked a highly lofted, extensive dust veil travelling across over eastern Asia, the Pacific Ocean, North America, and the Atlantic Ocean, which generated in an intensive dust storm occurring during 19–20 May 2007 in the Taklimakan Desert. By combining multiple observation datasets and analysis tools, we performed a comprehensive investigation on the dust emission and entrainment procedures over the source region to understand the generation mechanism of the dust veil as well as its subsequent intercontinental transport and 3-D structure.

The simulation results of the global SPRINTARS model showed a good agreement with the CALIOP measurements and revealed that the dust veil was transported at 4–10 km along the isentropic surface of 310–340 K with a thickness of 1–4 km. The SPRINTARS and HYSPLIT trajectory analyses estimated that the dust veil took 12 days (20–31 May) to travel from the Taklimakan Desert to the North Atlantic, yielding a trans-

port speed of  $\sim 1500$  km/d, consistent with the results of other studies. The dust amount exported into the Pacific Ocean was estimated to be 30.8 Gg. 65% of the dust loading was deposited in the Pacific Ocean and 18% was transported to the North Atlantic. This fact implied that, over the course of the intercontinental transport, the dust veil can fertilize the open oceans, contribute to the background dust in the free atmosphere, and affect the global radiative budget directly through scattering and absorbing the solar radiation.

The regional RC4 model with a better spatial resolution is used to analyze the emission and entrainment procedures of the dust veil over the source region, in combination with the passive satellite measurements and ground weather observations. During 19–20 May, strong northeasterly surface winds associated with a low pressure blew into the Tarim Basin through the east side corridor, kicking up large amounts of dust into the air. Meanwhile, strong updraft winds along the northern slope of the Tibetan Plateau formed, bringing airborne dust particles further up to the free troposphere (about 9 km MSL). The highly lofted dust particles in the free troposphere were then transported eastward by the westerly. The SYNOP surface weather observations recorded persistently low visibilities ( $< 1$  km) over the basin, indicating that the dust event was exceptionally intensive. Two mechanisms played the key role in the formation of the dust veil in the Taklimakan Desert. One is the presence in the basin of strong surface winds associated with low pressures, which can blow up massive amounts of dust into the atmosphere from the ground. The other one is the formation of a strong updraft by the high and steep mountainside of the Tibetan Plateau on the southern side of the basin. The strong updraft can entrain the suspended dust to the free troposphere, where westerlies are dominant. Figure 8 presents a schematic plot to summarize the emission and entrainment procedures of the dust veil over the Taklimakan Desert.

Over the course of the extraordinary long-range transport, the dust veil appeared to have affected the formation of ice clouds as the ice nuclei (Sakai et al. 2004; Sassen et al., 2003). The air masses along the dust transport track that satisfy the conditions of ice formation with the presence of mineral dust particles are denoted by gray-

## Elevated large-scale dust veil originated in the Taklimakan Desert

K. Yumimoto et al.

Title Page

Abstract

Introduction

Conclusions

References

Tables

Figures

⏪

⏩

◀

▶

Back

Close

Full Screen / Esc

Printer-friendly Version

Interactive Discussion

shaded areas in Figs. 2, 4 and 7. In these areas, relative humidity with respect to ice ( $RH_{ice}$ ) > 110%, and  $-35^{\circ}\text{C} < \text{temperature } (T) < -11^{\circ}\text{C}$  (Isono and Ikebe, 1960; Bailey and Hallett, 2002). These regions partly agree with the cloud regions classified by the CALIOP CAD index (Fig. 2), indicating a high possibility that the dust veil affects the ice cloud formation. Further analyses and observations are necessary to provide conclusive evidence especially for the interaction between dust and ice cloud.

*Acknowledgement.* This study was supported in part by the Research Fellowships of the Japan Society for the Promotion of Science (JSPS) for Young Scientists program (19-2611) and the Grant-in-Aid for Scientific Research in Priority Areas “Western Pacific Air-Sea Interaction Study (W-PASS)” under the Grant No. 18067009 from the Ministry of Education, Culture, Sports, Science and Technology (MEXT), Japan.

## References

- Aoki, I., Kurosaki, K., Osada, R., Sato, T., and Kimura, F.: Dust storms generated by mesoscale cold fronts in the Tarim Basin, Northwest China, *Geophys. Res. Lett.*, 32, L06807, doi:10.1029/2004GL021776, 2005.
- Bailey, M. and Hallett, J.: Nucleation effects on the habit of vapor grown ice crystal from  $-18$  to  $-42^{\circ}\text{C}$ , *Q. J. Roy. Meteorol. Soc.*, 128, 1461–1483, 2002.
- Bohren, C. F. and Huffman, D. R.: *Absorption and Scattering of Light by Small Particles*, John Wiley, New York, 1983.
- Bory, A. J.-M., Biscaye, P. E., and Grousset, F. E.: Two distinct seasonal Asian source regions for mineral dust deposited in Greenland (NorthGRIP), *Geophys. Res. Lett.*, 30(4), 1167, doi:10.1029/2002GL016446, 2003.
- Draxler, R. R. and Hess, G. D.: An overview of the HYSPLIT\_4 modeling system for trajectory, dispersion, and deposition, *Aust. Meteorol. Mag.*, 47, 295–308, 1998.
- Duce, R. A., Liss, C. K., Merrill, J. T., Atlas, E. L., Buat-Menard, P., Huck, B. B., Miller, J. M., Prospero, J. M., Arimoto, R., Church, T. M., Ellis, W., Galloway, J. N., Hassen, L., Jickells, T. D., Knap, A. H., and Reinhardt, K. H.: The atmospheric impact of trace species to the world ocean, *Glob. Biogeochem. Cy.*, 5, 193–259, 1991.

## Elevated large-scale dust veil originated in the Taklimakan Desert

K. Yumimoto et al.

Title Page

Abstract

Introduction

Conclusions

References

Tables

Figures

◀

▶

◀

▶

Back

Close

Full Screen / Esc

Printer-friendly Version

Interactive Discussion

- Eguchi, K., Uno, I., Yumimoto, K., Takemura, T., Shimizu, A., Sugimoto, N., and Liu, Z.: Trans-pacific dust transport: integrated analysis of NASA/CALIPSO and a global aerosol transport model, *Atmos. Chem. Phys.*, 9, 3137–3145, 2009, <http://www.atmos-chem-phys.net/9/3137/2009/>.
- 5 Fernald, F. G.: Analysis of atmospheric LIDAR observations: Some comments, *Appl. Opt.*, 23, 652–653.
- Generoso, S., Bey, I., Labonne, M., and Bréon, F.-M.: Aerosol vertical distribution in dust outflow over the Atlantic: Comparisons between GEOS-Chem and Cloud–Aerosol Lidar and Infrared Pathfinder Satellite Observation (CALIPSO), *J. Geophys. Res.*, 113, D24209, doi:10.1029/2008JD010154, 2008.
- 10 Grousset, F. E., Ginoux, P., Bory, A., and Biscaye, P. E.: Case study of a Chinese dust plume reaching the French Alps, *Geophys. Res. Lett.*, 30(6), 1277, doi:10.1029/2002GL016833, 2003.
- Kurosaki, Y. and Mikami, M.: Recent frequent dust events and their relation to surface wind in East Asia, *Geophys. Res. Lett.*, 30(14), 1736, doi:10.1029/2003GL017261, 2003.
- K-1 Model Developers: K-1 coupled GCM (MIROC) description, K-1 Tech. Rep. 1, edited by Haumi, H. and Emori, E., Univ. of Tokyo, Tokyo, 2004.
- Hara, Y., Uno, I., Yumimoto, K., Tanaka, M., Shimizu, A., Sugimoto, N., and Liu, Z.: Summertime Taklimakan dust structure, *Geophys. Res. Lett.*, 35, L23801, doi:10.1029/2008JD035630, 2008.
- 20 Hara, Y., Yumimoto, K., Uno, I., Shimizu, A., Sugimoto, N., Liu, Z., and Winker, D. M.: Asian dust outflow in the PBL and free atmosphere retrieved by NASA CALIPSO and an assimilated dust transport model, *Atmos. Chem. Phys.*, 9, 1227–1239, 2009, <http://www.atmos-chem-phys.net/9/1227/2009/>.
- 25 Husar, R. B., Tratt, D. M., Schichtel, B. A., et al.: Asian dust events of April 1998, *J. Geophys. Res.*, 106(D16), 18317–18330, 2001.
- Huang, J., Minnis, P., Chen, B., Huang, Z., Liu, Z., Zhao, Q., Yi, Y., and Ayers, J. K.: Long-range transport and vertical structure of Asian dust from CALIPSO and surface measurements during PACDEX, *J. Geophys. Res.*, 113, D23212, doi:10.1029/2008JD010620, 2008.
- 30 Isono, K. and Ikebe, Y.: On the ice-nucleating ability of rock-forming minerals and soil particles, *J. Meteorol. Soc. Jpn.*, 38, 211–233, 1960.
- Liu, Z., Liu, D., Huang, J., Vaughan, M., Uno, I., Sugimoto, N., Kittaka, C., Trepte, C., Wang, Z., Hostetler, C., and Winker, D.: Airborne dust distributions over the Tibetan Plateau and sur-

---

## Elevated large-scale dust veil originated in the Taklimakan Desert

K. Yumimoto et al.

---

Title Page

Abstract

Introduction

Conclusions

References

Tables

Figures

⏪

⏩

◀

▶

Back

Close

Full Screen / Esc

Printer-friendly Version

Interactive Discussion

rounding areas derived from the first year of CALIPSO lidar observations, *Atmos. Chem. Phys.*, 8, 5045–5060, 2008a,

<http://www.atmos-chem-phys.net/8/5045/2008/>.

Liu, Z., Omar, A., Vaughan, M., Hair, J., Kittaka, C., Hu, Y., Powell, K., Trepte, C., Winker, D., Hostetler, C., Ferrare, R., and Pierce, R.: CALIPSO lidar observations of the optical properties of Saharan dust: A case study of long-range transport, *J. Geophys. Res.*, 113, D07207, doi:10.1029/2007JD008878, 2008b.

Martin, J. H., Coale, K. H., Johnson, K. S., et al.: Testing the iron hypothesis in ecosystems of the equatorial Pacific Ocean, *Nature* 371, 123–129, 1994.

Matsuki, A., Iwasaka, Y., Osada, K., et al.: Seasonal dependence of the long-range transport and vertical distribution of free tropospheric aerosols over east Asia: On the basis of aircraft and lidar measurements and isentropic trajectory analysis, *J. Geophys. Res.*, 108(D23), 8663, doi:10.1029/2002JD003266, 2003.

McKendry, I. G., Hacker, J. P., Stull, R., Sakiyama, S., Mignacca, D., and Reid, K.: Long-range transport of Asian dust to the Lower Fraser Valley, British Columbia, Canada, *J. Desert Res.*, 106, 18361–18370, 2001.

Prospero, J. M., Ginoux, P., Torres, O., Nicholson, S. E., and Gill, T. E.: Environmental characterization of global sources of atmospheric soil dust identified with the NIMBUS 7 Total Ozone Mapping Spectrometer (TOMS) absorbing aerosol product, *Rev. Geophys.*, 40(1), 1002, doi:10/1029/2000RG000095, 2002.

Sakai, T., Nagai, T., Nakazawa, M., and Matsumura, T.: Raman lidar measurement of water vapor and ice clouds associated with Asian dust layer over Tsukuba, Japan, *Geophys. Res. Lett.*, 31, L06128, doi:10.1029/2003GL019332, 2004.

Shimizu, A., Sugimoto, N., Matsui, I., Tatarov, B., Xie, C., Nishizawa, T., and Hara, Y.: NIES lidar Network; strategies and applications, 24rd International Laser Rader Conference, 23–28 June 2008, Boulder, CO, USA, (24ILRC, ISBN 978-0-615-21489-4), 707–710, 2008.

Shimizu, A., Sugimoto, N., Matsui, I., Arao, K., Uno, I., Murayama, T., Kagawa, N., Aoki, K., Uchiyama, A., and Yamazaki, A.: Continuous observations of Asian dust and other aerosols by polarization lidars in China and Japan during ACE–Asia, *J. Geophys. Res.*, 109, D19S17, doi:10.1029/2002JD003253, 2004.

Sun, J., Chang, M., and Liu, T.: Spatial and temporal characteristics of dust storms in China and its surrounding regions, 1960–1999: Relations to source area and climate, *J. Geophys. Res.*, 106, 18331–18344, 2001.

ACPD

9, 14453–14481, 2009

## Elevated large-scale dust veil originated in the Taklimakan Desert

K. Yumimoto et al.

Title Page

Abstract

Introduction

Conclusions

References

Tables

Figures

◀

▶

◀

▶

Back

Close

Full Screen / Esc

Printer-friendly Version

Interactive Discussion

---

**Elevated large-scale  
dust veil originated in  
the Taklimakan  
Desert**K. Yumimoto et al.

---

[Title Page](#)[Abstract](#)[Introduction](#)[Conclusions](#)[References](#)[Tables](#)[Figures](#)[⏪](#)[⏩](#)[◀](#)[▶](#)[Back](#)[Close](#)[Full Screen / Esc](#)[Printer-friendly Version](#)[Interactive Discussion](#)

Sussen, K., DeMott, P. J., Prospero, J. M., and Poellot, M. R.: Sagarán dust storms and indirect aerosol effect on clouds: CRYSTAL-FACE results, *Geophys. Res. Lett.*, 30(12), 1633, doi:10.1029/2003GL017371, 2003.

Takemura, T., Nozawa, T., Emori, S., Nakajima, T. Y., and Nakajima, T.: Simulation of climate response to aerosol direct and indirect effect with aerosol transport-radiation model, *J. Geophys. Res.*, 110, D02202, doi:10.1029/2004JD005029, 2005.

Tegen, I. and Fung, I.: Modeling of mineral dust in the atmosphere: Sources, transport, and optical thickness, *J. Geophys. Res.*, 99, 22897–22914, 1994.

Twomey, S.: The influence of pollution on the shortwave albedo of clouds, *J. Atmos. Sci.*, 34(7), 1149–1154, 2002.

Uno, I., Satake, S., Carmichael, G. R., et al.: Numerical study of Asian dust transport during the springtime of 2001 simulated with the Chemical Weather Forecasting System (CFORS) model, *J. Geophys. Res.*, 109, D19S24, doi:10.1029/2003JD00422, 2004.

Uno, I., Harada, K., Satake, S., Hara, H., and Wang, Z.: Meteorological characteristics and dust distribution of the Tarim Basin simulated by the nesting RAMS/CFORS dust model, *J. Meteorol. Soc. Japan*, 83A, 219–239, 2005.

Uno, I., Yumimoto, K., Shimizu, A., Hara, Y., Sugimoto, N., Wang, Z., Liu, Z., and Winker, D. M.: 3-D Structure of Asian Dust Transport revealed by CALIPSO Lidar and a 4DVAR Dust Model, *Geophys. Res. Lett.*, 35, L06803, doi:10.1029/2007GL032329, 2008.

Yu, H., Dickinson, R. E., Chin, M., Kaufman, Y. J., Holben, B. N., Geogdzhayev, I. V., and Mishchenko M. I.: Annual cycle of global distribution of aerosol optical depth from integration of MODIS retrievals and GOCART model simulation, *J. Geophys. Res.* 108(D3), 4128, doi:10.1029/2002JD002717, 2003.

Yumimoto, K., Uno, I., Sugimoto, N., Shimizu, A., and Satake, S.: Adjoint inversion modelling of dust emission and transport over East Asia, *Geophys. Res. Lett.* 34, L08806, doi:10.1029/2006GL028551, 2007.

Yumimoto, K., Uno, I., Sugimoto, N., Shimizu, A., Liu, Z., and Winker, D. M.: Adjoint inversion modeling of Asian dust emission using lidar observations, *Atmos. Chem. Phys.*, 8, 2869–2884, 2008, <http://www.atmos-chem-phys.net/8/2869/2008/>.

Winker, D. M., Hunt, W. H., and McGill, M. J.: Initial performance assessment of CALIOP, *Geophys. Res. Lett.* 34, L19803, doi:10.1029/2007GL030135, 2007.

## Elevated large-scale dust veil originated in the Taklimakan Desert

K. Yumimoto et al.

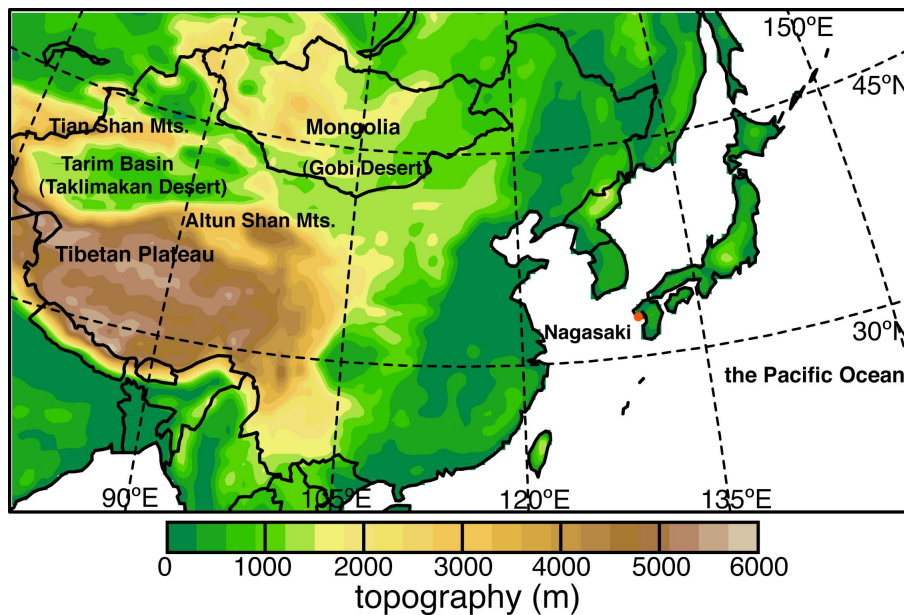


**Fig. 1.** The RC4 modeling domain and topography of the Taklimakan Desert.

Title Page

Abstract

Introduction

Conclusions

References

Tables

Figures

◀

▶

◀

▶

Back

Close

Full Screen / Esc

Printer-friendly Version

Interactive Discussion

## Elevated large-scale dust veil originated in the Taklimakan Desert

K. Yumimoto et al.

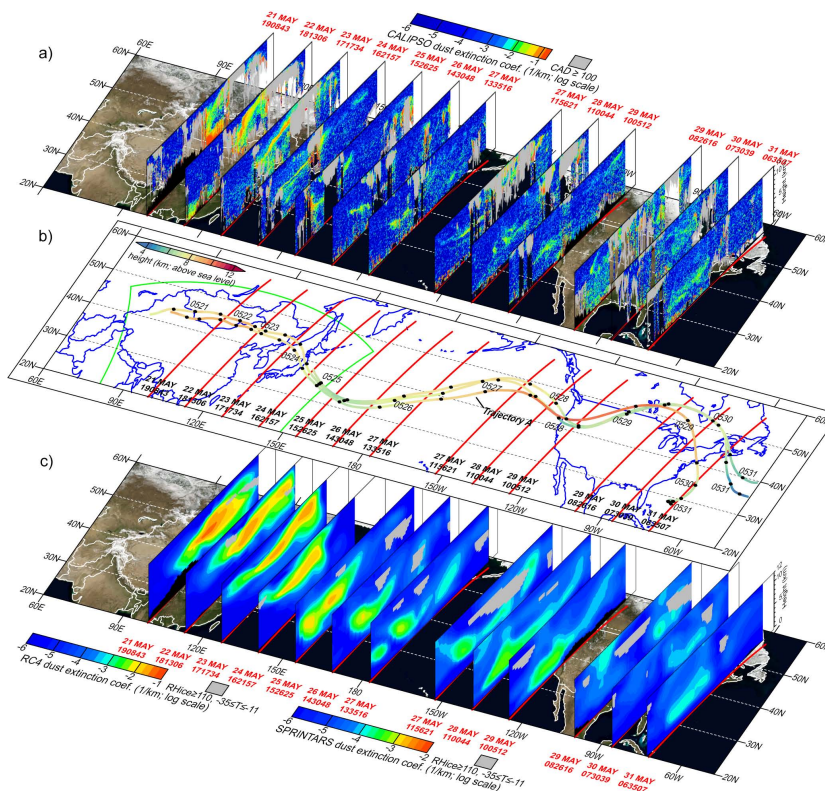


**Fig. 2.** Three-dimensional analysis of intercontinental transport of the dust veil. **(a)** Cross-sections of the CALIPSO dust extinction coefficient with the cloudy regions shaded in gray ( $CAD > 100$ ). **(b)** HYSPLIT forward and backward trajectories started at 17:00 UTC on 24 May at  $36\text{--}38^\circ\text{N}$  and  $145\text{--}146^\circ\text{E}$  and 7000 m above sea level on the 24 May-162157 CALIPSO orbit. The colors represent different trajectory heights. The region surrounded by the green lines represents the RC4 model domain. **(c)** Cross-sections of the model simulated dust extinction coefficient. The first four cross-sections over eastern Asia during 21–24 May are simulated by the RC4 model and the rest are derived from the SPRINTARS model. Shaded areas in gray represent regions that satisfy the condition of heterogeneous ice formation for mineral dust particles: relative humidity with respect to ice ( $RH_{ice}$ )  $> 110\%$ , and  $-35^\circ\text{C} < \text{temperature } (T) < -11^\circ\text{C}$ .

Title Page

Abstract

Introduction

Conclusions

References

Tables

Figures

⏪

⏩

◀

▶

Back

Close

Full Screen / Esc

Printer-friendly Version

Interactive Discussion

## Elevated large-scale dust veil originated in the Taklimakan Desert

K. Yumimoto et al.

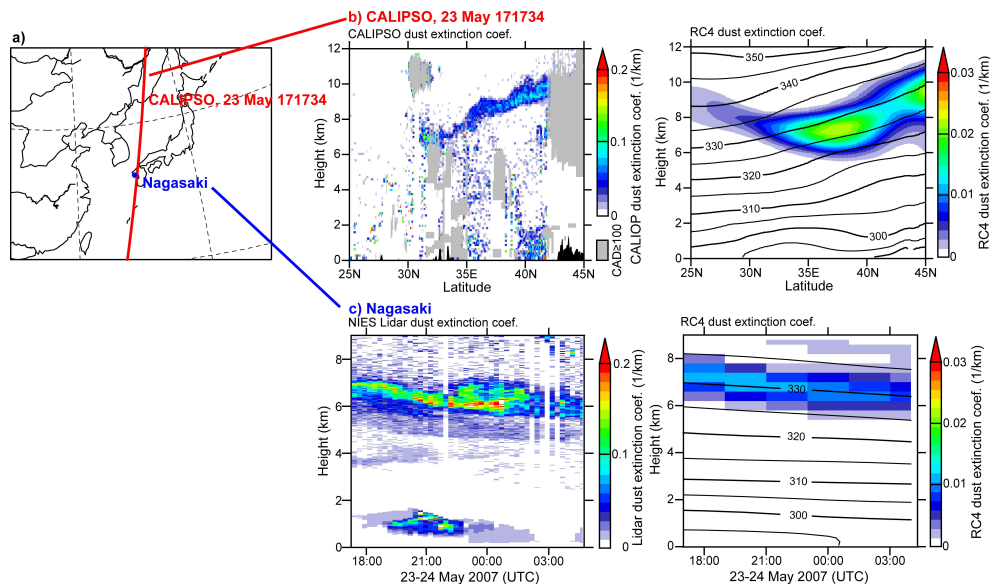


**Fig. 3.** Comparison of measured and simulated dust extinction coefficients. **(a)** CALIPSO orbit path and location of the Nagasaki Lidar site; **(b)** cross-sections of the CALIOP measured and the RC4 simulated dust extinction coefficients along the CALIPSO orbit shown in (a); **(c)** time-height cross-sections of the NIES Lidar measured and the RC4 simulated dust extinction coefficients at the Nagasaki lidar site. Black counter lines in the right panels represent the RC4 potential temperature.

Title Page

Abstract

Introduction

Conclusions

References

Tables

Figures

◀

▶

◀

▶

Back

Close

Full Screen / Esc

Printer-friendly Version

Interactive Discussion

## Elevated large-scale dust veil originated in the Taklimakan Desert

K. Yumimoto et al.

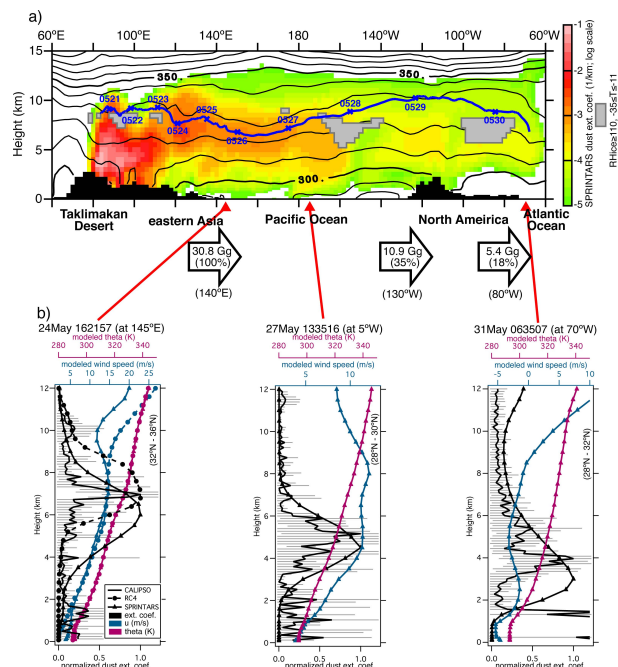


**Fig. 4.** (a) Vertical-longitudinal cross-section of the SPRINTARS simulated dust extinction coefficient along the HYSPLIT trajectory denoted by “trajectory A” in Fig. 1b. Modeled potential temperature (black contours) and the HYSPLIT trajectory (blue line) are also shown. Shaded areas in gray represent regions that satisfy the condition of heterogeneous ice formation for mineral dust particles: relative humidity with respect to ice ( $RH_{ice}$ ) > 110%, and  $-35^{\circ}\text{C} < \text{temperature } (T) < -11^{\circ}\text{C}$ . Horizontal dust fluxes at  $140^{\circ}\text{E}$ ,  $130^{\circ}\text{W}$  and  $80^{\circ}\text{W}$  estimated by SPRINTARS are shown by the numbers in the arrows, where the percentage number in each bracket representing the ratio of the dust amount to that exported to the Pacific through the  $140^{\circ}\text{E}$  meridian plan. (b) Normalized vertical profiles of dust extinction coefficient measured by CALIOP (solid lines) and simulated by RC4 (broken lines with solid circles) and SPRINTARS (solid lines with triangles), along the 24 May-162157, 27 May-133516, and 31 May-063507 CALIOP orbits, respectively. Horizontal error bars represent  $\pm 1\sigma$  of the CALIOP observations. Modeled east–west wind speed and potential temperature are also shown as blue and red profiles. Each profile is calculated by latitudinal average: averaged regions are given in the panels by latitude.

Title Page

Abstract

Introduction

Conclusions

References

Tables

Figures

◀

▶

◀

▶

Back

Close

Full Screen / Esc

Printer-friendly Version

Interactive Discussion

## Elevated large-scale dust veil originated in the Taklimakan Desert

K. Yumimoto et al.

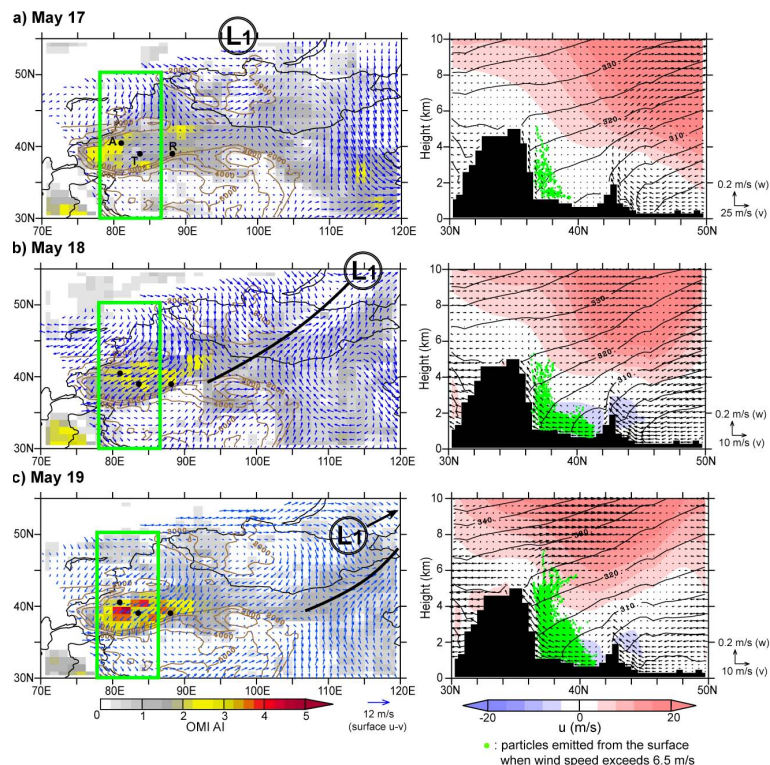


**Fig. 5.** Detailed analysis for the emission and entrainment procedures of dust over the source region to form the dust veil. Left panels show the OMI AI (color), the RC4 simulated daily averaged surface wind vectors (blue vectors), and the topography (brown contours). The locations of low pressures (circled character L) and associated cold front (solid black lines) which are estimated by the pressure on mean sea level from the  $2.5^\circ \times 2.5^\circ$  NCEP/NCAR reanalysis (not shown), the MODIS true color image (also see Fig. 7) and the RC4 results, are also shown. Right panels portray the averaged cross-sections for the regions as indicated by the green rectangles in the left panels. Green dots represent the results of the particle simulation. Colored contours depict the daily averaged wind speed in the east–west direction. Black contours represent the daily averaged potential temperatures. The SYNOP observation stations are also shown in (a) by black solid circles: Alar (A:  $81.1^\circ$  E,  $40.5^\circ$  N), Tazhong (T:  $83.7^\circ$  E,  $39.0^\circ$  N), and Ruoqiang (R:  $88.2^\circ$  E,  $39.0^\circ$  N).

Title Page

Abstract

Introduction

Conclusions

References

Tables

Figures

◀

▶

◀

▶

Back

Close

Full Screen / Esc

Printer-friendly Version

Interactive Discussion

## Elevated large-scale dust veil originated in the Taklimakan Desert

K. Yumimoto et al.

Title Page

Abstract

Introduction

Conclusions

References

Tables

Figures

◀

▶

◀

▶

Back

Close

Full Screen / Esc

Printer-friendly Version

Interactive Discussion

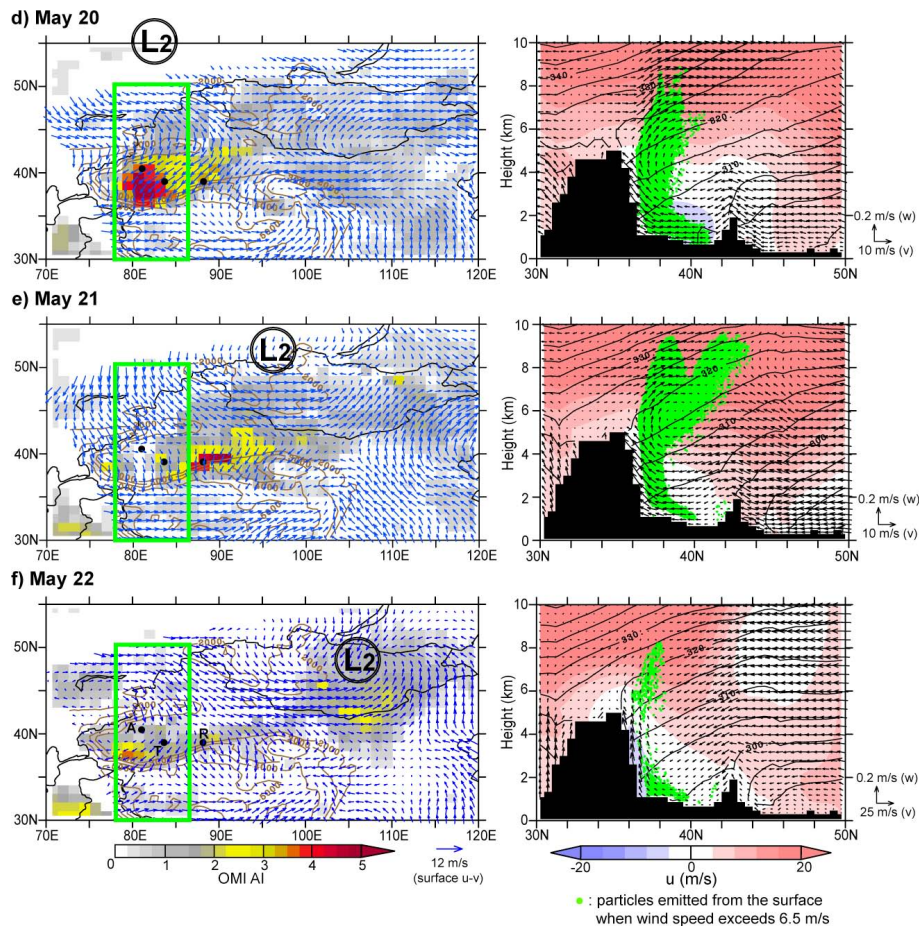
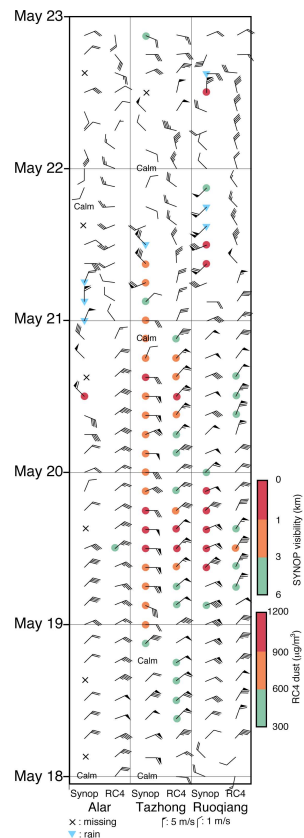


Fig. 5. Continued.

## Elevated large-scale dust veil originated in the Taklimakan Desert

K. Yumimoto et al.



**Fig. 6.** Time series of the SYNOP observed and the RC4 simulated surface wind speed and direction during 18–21 May at Alar (located at the northern part of the desert), Tazhong (central part), and Ruoqiang (eastern part). Visibility and rain events are shown as symbols. The RC4 simulated surface dust concentrations are also shown.

Title Page

Abstract

Introduction

Conclusions

References

Tables

Figures

◀

▶

◀

▶

Back

Close

Full Screen / Esc

Printer-friendly Version

Interactive Discussion

## Elevated large-scale dust veil originated in the Taklimakan Desert

K. Yumimoto et al.

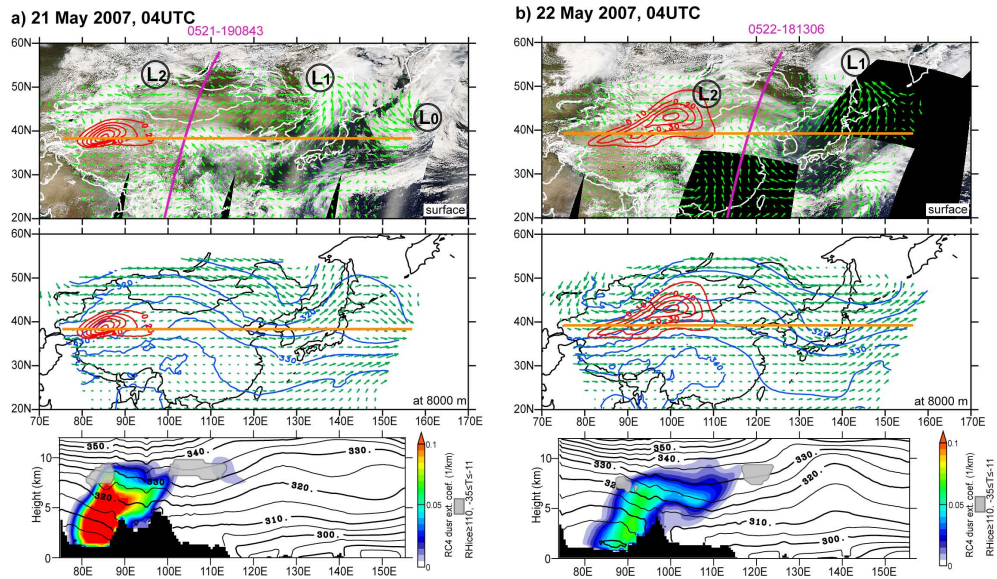


**Fig. 7.** Day-by-day overview of daily evolution of the dust veil transport during 21 to 24 May. Upper panels show horizontal distributions of the modeled Aerosol Optical Depth (AOD) (red contours) and wind fields (green vectors) at the surface at 04:00 UTC. Pink lines show the CALIPSO orbit paths. Also shown are the MODIS/Aqua RGB color composite cloud images, the locations of low pressures and cold fronts at the ground surface. Middle panels depict the modeled wind (green vectors) and potential temperature (blue lines) at the RC4 25th layer (~8 km MSL). Lower panels show cross-sections, along the orange lines in the upper two panels, of the RC4 simulated dust extinction coefficient (color contour), potential temperature (black line), and the regions that satisfy the condition of heterogeneous ice formation for mineral dust particles: relative humidity with respect to ice ( $RH_{ice}$ ) > 110%, and  $-35^{\circ}\text{C} < \text{temperature } (T) < -11^{\circ}\text{C}$  (gray shading).

Title Page

Abstract

Introduction

Conclusions

References

Tables

Figures

◀

▶

◀

▶

Back

Close

Full Screen / Esc

Printer-friendly Version

Interactive Discussion

**Elevated large-scale  
dust veil originated in  
the Taklimakan  
Desert**

K. Yumimoto et al.

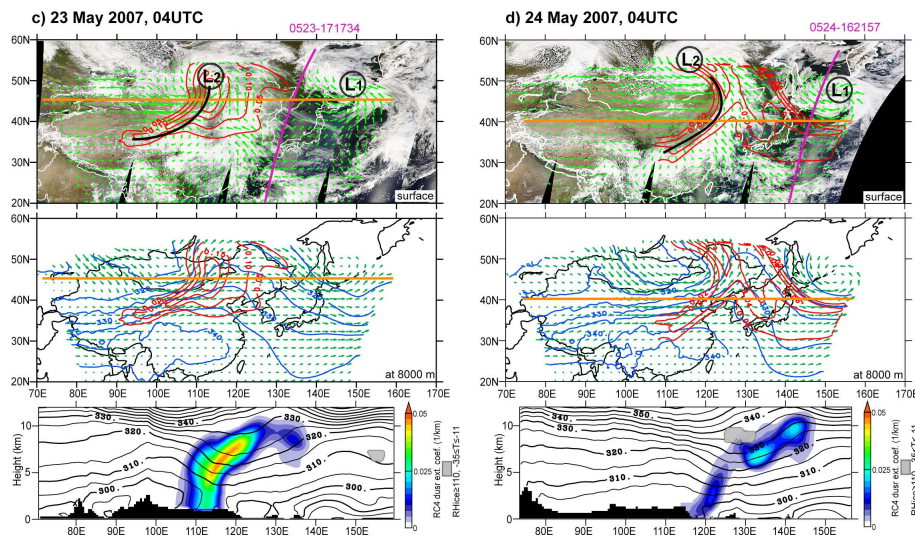
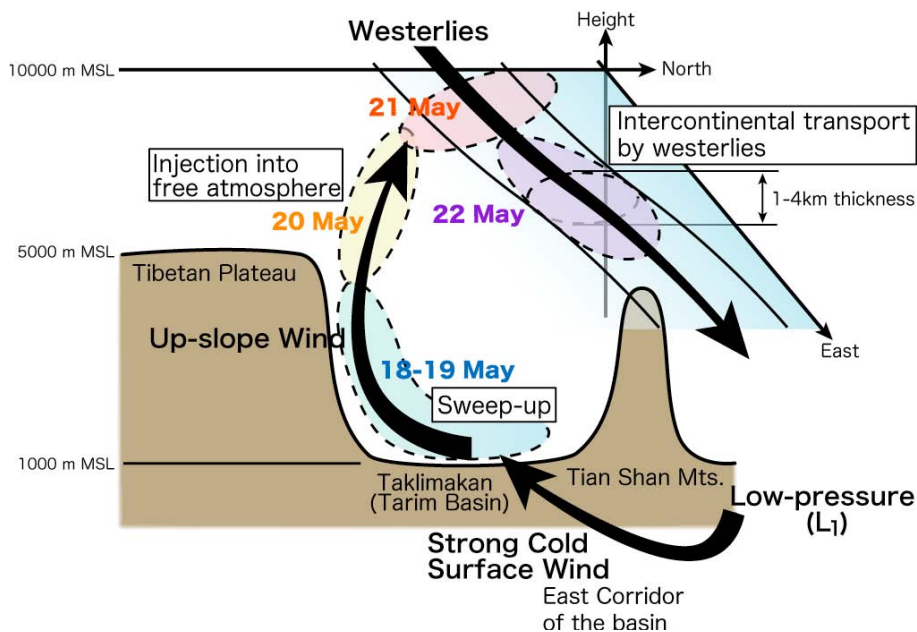


Fig. 7. Continued.

[Title Page](#)[Abstract](#)[Introduction](#)[Conclusions](#)[References](#)[Tables](#)[Figures](#)[⏪](#)[⏩](#)[◀](#)[▶](#)[Back](#)[Close](#)[Full Screen / Esc](#)[Printer-friendly Version](#)[Interactive Discussion](#)

## Elevated large-scale dust veil originated in the Taklimakan Desert

K. Yumimoto et al.



**Fig. 8.** Schematic of the emission and entrainment processes of dust over the Taklimakan Desert (Tarim Basin) to form the dust veil.

Title Page

Abstract

Introduction

Conclusions

References

Tables

Figures

◀

▶

◀

▶

Back

Close

Full Screen / Esc

Printer-friendly Version

Interactive Discussion